Biochemistry

 Volume 31, Number 3 January 28, 1992

Articles

Polymyxin B Induces Transient Permeability Fluctuations in Asymmetric Planar Lipopolysaccharide/Phospholipid Bilayers†

Guido Schröder, Klaus Brandenburg, and Ulrich Seydel*
Division of Biophysics, Forschungsinstitut Borstel, D-2061 Borstel, Germany
Received July 23, 1991; Revised Manuscript Received October 15, 1991

ABSTRACT: The interaction of the polycationic decapeptide polymyxin B with asymmetric planar bilayers from lipopolysaccharide and phospholipid monolayers, which resemble the lipid matrix of the outer membrane of Gram-negative bacteria, was investigated. The addition of polymyxin B in micromolar amounts to the lipopolysaccharide side of the asymmetric bilayers resulted, under voltage-clamp conditions, in a fast macroscopic increase of their ionic conductance, whereas the polymyxin B nonapeptide induced no significant conductance changes. The polymyxin B induced macroscopic conductance exhibited large fluctuations and was strongly dependent on the amplitude and polarity of the transmembrane potential. The temporal pattern and amplitudes of the fluctuations were characterized by power spectra of the membrane currents and their variances, respectively. In the initial phase following peptide addition, the conductance changes appeared to be channellike discrete fluctuations. The lifetimes of the fluctuations were exponentially distributed, and the mean lifetimes were strongly voltage-dependent, ranging from approximately 30 ms at +80 mV (positive at the side opposite to peptide addition) to less than 5 ms at reverse polarity. The conductance amplitudes of the single fluctuations exhibited a broad distribution with a mean of 2 nS. A comparison of the features of the macroscopic conductance and of the discrete fluctuations showed that the former can basically be understood as a superposition of a large number of the latter. From the amplitudes of the fluctuations, the diameter of the polymyxin-induced lesions was estimated to about 3 nm. The experimental findings can be understood by assuming a detergent-like action of polymyxin B.

The polycationic decapeptide polymyxin B (PMB),[1] which is built up from a cyclic heptapeptide moiety linked to a peptide side chain which terminates with a short fatty acid residue, exerts antibiotic activity against most genera of Gram-negative bacteria including *Escherichia*, *Salmonella*, or *Pseudomonas* at minimal inhibitory concentrations less than 2 μg/mL (Storm & Rosenthal, 1977). The primary target of PMB was shown to be the outer membrane of these bacteria (Vaara & Vaara, 1983a) which undergoes a rapid increase of the membrane permeability with respect to charged or polar molecules of low molecular weight (Teuber, 1974) and visible morphological alterations (Schindler & Teuber, 1975).

The activity of PMB on biological membranes has also been established with various model membrane systems such as lipid monolayers (Theretz et al., 1984; Beurer et al., 1988), liposomal membranes (HsuChen & Feingold, 1973; Imai et al., 1975; Ranck & Tocanne, 1982; Mushayakarara & Levin, 1984; Sixl & Watts, 1985; Beurer et al., 1988), and black lipid membranes (BLM's)[1] (Antonov et al., 1976; Miller et al., 1978), and a variety of physical techniques such as electron spin resonance (ESR),[1] nuclear magnetic resonance (NMR),[1] fluorescence polarization, calorimetric methods, and X-ray diffraction were applied. As should be expected from the polycationic character of PMB (under physiological conditions, it carries five positive charges), strong interactions have been observed with negatively charged amphiphiles including phospholipids (PL's)[1] like phosphatidic acid (PA)[1] (Kubesch

†Supported by the Deutsche Forschungsgemeinschaft (Grant Se 532/2-1).

[1] Abbreviations: LPS, lipopolysaccharide; PMB, polymyxin B; PMBN, polymyxin B nonapeptide; PL, phospholipid; PC, phosphatidylcholine; PE, phosphatidylethanolamine; PS, phosphatidylserine; PG, phosphatidylglycerol; CL, cardiolipin; BLM, black lipid membrane; NMR, nuclear magnetic resonance; ESR, electron spin resonance.

0006-2960/92/0431-631$03.00/0

et al., 1987) or phosphatidylglycerols (PG's)[1] (Boggs & Rangaraj, 1985) and, particularly, lipopolysaccharides (LPS's)[1] (Schindler & Teuber, 1975; Schindler & Osborn, 1979; Peterson et al., 1985). The latter compounds are the major amphiphilic constituents of the outer leaflet of the outer membrane of Gram-negative bacteria.

Out of the number of applied techniques, NMR, ESR, X-ray diffraction, and calorimetric measurements supplied mainly structural information, i.e., binding properties of PMB to lipids, its distribution in the lipid matrix, and fluidity changes. Information on the nature of the PMB-induced permeability increase was provided by investigations with liposomes and planar membranes applying optical or electrical techniques for transport measurements. Thus, the release of glucose (HsuChen & Feingold, 1973; Imai et al., 1975) and of carboxyfluorescein (Kubesch et al., 1987) entrapped in liposomes has been demonstrated. From measurements of the electrical conductivity of planar lipid bilayers, contradictory results were obtained. Antonov et al. (1976) used neutral lecithin BLM's which they charged by the addition of ionic detergents. From the observed changes in electrical conductivity, they proposed a carrier mechanism for the action of PMB. In contrast, Miller et al. (1978) found that the electrical resistance of BLM's made exclusively from phosphatidylserine (PS)[1] or from mixtures of phosphatidylethanolamine (PE)[1] and PG was not affected by PMB. They observed only an unspecific destabilization of the membranes.

In summary, it may be concluded that the detailed mechanisms of the interaction between PMB and bacterial outer membranes on the molecular level are still poorly understood, especially with respect to the permeability changes induced in the outer membrane.

This study reports on the action of PMB and the polymyxin B nonapeptide (PMBN),[1] which lacks the terminal diaminobutyric acid and the fatty acid residue of PMB, on an asymmetric planar membrane system reconstituting the lipid matrix of the outer membrane of rough mutant strains of Gram-negative bacteria, which are known to be most sensitive to PMB. It is built up on one side exclusively from deep rough mutant LPS and on the other side from a PL mixture.

Under voltage-clamp conditions, discrete channellike changes in the ionic conductance of the planar bilayers after addition of PMB—but not of PMBN—were detected. Thus, it was possible to study directly the breakdown of the outer membrane permeability barrier and to estimate the size of the PMB-induced lesions.

On the basis of the observed conductivity fluctuations, a model for the action of PMB on the lipid bilayer is proposed which is related to that of detergents. According to this model, the fluctuations are induced either by pure PMB or by mixed PMB/lipid micelles.

Materials and Methods

Materials

As LPS, that of *Salmonella minnesota* strain R595 containing only lipid A and two 2-keto-3-deoxyoctonate (KDO) monosaccharides was used (Figure 1). It was extracted by the phenol/chloroform/petrol ether method (Galanos et al., 1969) and lyophilized. As phospholipids, PG from egg yolk lecithin (sodium salt), phosphatidylcholine (PC)[1] from bovine brain (type III-B), or a mixture of PE from *Escherichia coli* (type V), PG, and cardiolipin (CL)[1] from bovine heart (sodium salt) in a molar ratio of 81:17:2 (PE/PG/CL) were used. The mixture resembles the PL composition of the inner leaflet of the outer membrane of *Salmonella typhimurium* (Osborn et al., 1972). All PL's and PMB were purchased from Sigma (Deisenhofen, Germany); PMBN was from Boehringer (Mannheim, Germany). The chemical structure of the peptides is given in Figure 2.

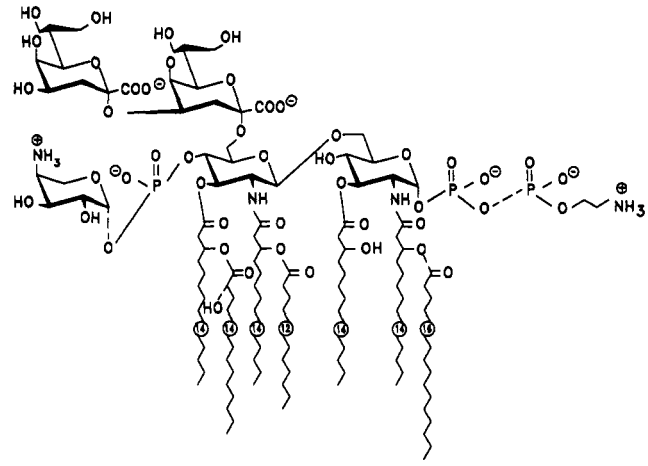

FIGURE 1: Chemical structure of LPS from *S. minnesota* deep rough mutant strain R595. The dashed lines indicate a nonstoichiometric substitution.

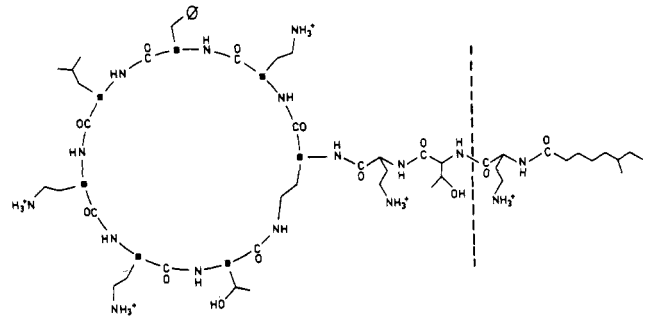

FIGURE 2: Chemical structure of PMB and PMBN. PMBN differs from PMB in that the terminal fatty acid and diaminobutyric acid are cleaved (dashed line).

Methods

Asymmetric Planar Bilayers and Electrical Measurements. The preparation of solvent-free asymmetric planar lipopolysaccharide/phospholipid bilayers has been described (Seydel et al., 1989). Briefly, asymmetric bilayers are formed by apposing monolayers prepared on two aqueous subphases from chloroform solutions of LPS and PL, respectively, at a small aperture punched into a thin Teflon foil (12.5-μm thickness). Clear solutions of R595 LPS in chloroform/methanol (9:1 by volume) were obtained by heating the suspension to 80 °C for 5 min. Diameters of the apertures were typically 200 μm, and the Teflon foil was pretreated with a 20:1 (v/v) hexane/hexadecane solution. Membrane currents were measured under voltage-clamping at a bandwidth of 800 Hz. Voltage signs refer to the compartment virtually grounded by the operational amplifier. Current is defined positive when the cations flow into the virtually grounded compartment. The output of the voltage clamp either was stored on a digital audio tape recorder (300ES, Sony) with a bandwidth extended to zero frequency by various modifications of the input stage, similar to those described by Bezanilla (1985), or was sampled directly during the experiments with a microcomputer system. For analysis, current signals were low-pass-filtered at 700 Hz (−3-dB point) (Ithaco Model 4302, New York), amplified by factors of 1, 10, or 100, and digitized at the indicated rates with a PCI-20089W-1 analog input board (Burr Brown, Filderstadt, Germany) plugged into an AT-compatible mi-

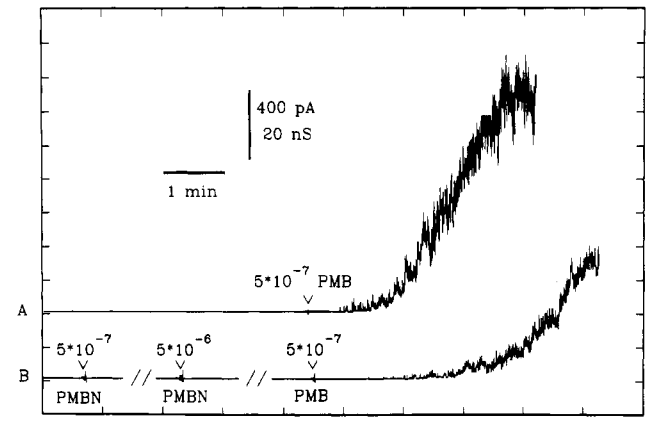

FIGURE 3: Time course of membrane currents for asymmetric LPS/PG bilayers at constant applied voltage (+20 mV at the side opposite to peptide addition) after addition of PMB or PMBN, respectively, to the LPS side of the bilayers. Double bars represent silent periods of 5 min with no significant changes of the current. Trace A: addition of PMB to the LPS side of an asymmetric LPS/PG bilayer. Trace B: addition of PMBN to the LPS side of an asymmetric LPS/PG bilayer followed by the addition of PMB to the same side.

crocomputer system. Spectral power densities were estimated by averaging fast Fourier-transforms of segments with 4096 points of digitized data sampled at 1 kHz. For the characterization of discrete fluctuations, signals were sampled at a rate of 4 kHz. All experiments were performed at 37 °C with membrane bathing solutions (subphases) containing 5 mM $MgCl_2$ (Mg^{2+} is present also in the natural system and serves for membrane stabilization), 5 mM Hepes, and 100 mM KCl at pH 7. The unmodified membranes exhibited a basic conductance not exceeding 50 pS at 20-mV clamp voltage, were stable up to several hours, and showed no channellike conductance fluctuations. The peptides were added in aliquots of 10 μL to the LPS side of the membranes which was virtually grounded by the feedback amplifier. After addition of the peptide, the bathing solutions were stirred for 30 s with magnetic bars.

Film Balance Measurements. To study the incorporation of PMB and PMBN into LPS monolayers, pressure–area isotherms were measured with a thermostated film balance (Krüss, Hamburg, Germany) on aqueous subphases containing 0.1 M NaCl and varying amounts of PMB and PMBN, respectively. The measurements were performed according to a protocol by Beurer et al. (1988). Briefly, the chloroform solutions of LPS were spread on the subphase and allowed to equilibrate for solvent evaporation, then compressed to 20 mN m^{-1} and held at that pressure for 30 min, expanded again, and equilibrated for another 30 min. After this procedure, the final isotherm was registered at room temperature.

RESULTS

Macroscopic Conductance Changes. Figure 3 trace A shows that addition of PMB at physiological concentrations (5×10^{-7} M) to the LPS side increases the ionic conductance of the asymmetric planar LPS/PG bilayer systems by several orders of magnitude. The transmembrane potential was clamped to +20 mV. Typically, within 1 min after addition of the peptide, a rapid increase of the transmembrane current was observed. In the immediate phase following PMB addition, channellike fluctuations of the bilayer conductance set on, which after a few minutes turned into a new steady state with large current fluctuations. The initial channel-like fluctuations are characterized in detail in the following section. Under the conditions defined above, membranes were significantly destabilized and frequently broke down before the current reached a stationary phase. Similar slopes of the current increase as in Figure 3 were registered in multiple experiments performed under identical conditions. However, in a few experiments, a considerably slower increase of the conductance was observed; i.e., in these experiments, the periods with discrete fluctuations lasted up to several minutes. Since the discrete fluctuations in these experiments showed essentially the same behaviour as those in experiments with a fast conductance increase, they were used to study the fluctuations over prolonged periods (see for example Figure 10).

Repeated addition of PMB to the same side in the steady state resulted in no significant changes of the current signal.

The peptide concentration required to induce the described effects was very critical. Successive increase of the PMB concentration to a final value of 2.5×10^{-7} M resulted only in minor changes in the current but influenced the stability of the membranes, leading in many cases to unspecific breakdown. Beyond this value, the membranes could withstand relatively large concentrations up to 10^{-5} M, whereas the addition of PMB in one step at final concentrations above approximately 10^{-6} M always resulted in fast membrane breakdown.

Essentially the same effects were observed with membranes with the PL side either composed of the PL mixture or composed exclusively of PC. However, these systems more often broke down before equilibrium states were reached, thus impeding their detailed investigation.

Since chemical alterations of the peptide could possibly reveal valuable information on the mechanisms of action of PMB, we also tested its nonapeptide PMBN, lacking the terminal diaminobutyric acid and the fatty acid residue. Figure 3 trace B shows that the addition of PMBN did not result in detectable alterations of the membrane conductivity. Subsequent addition of PMB to PMBN-pretreated membranes led to similar effects as observed for the addition of PMB alone. However, under these conditions, the temporal development of the macroscopic conductance increase seemed to be slower.

Switching the clamp voltage across the membrane in the steady state (as described above) after addition of the peptide revealed a marked voltage dependence of the macroscopic conductance of the PMB-treated bilayers (Figure 4). Upon switching from positive (on the side of the peptide-free compartment) to negative polarity, the current changed sign abruptly and then declined exponentially within seconds to a new steady-state current which was considerably lower than at the same voltage but of reverse polarity. Half-times of the exponential decline decreased with increasing negative potentials from 4.2 ± 0.2 s at −20 mV to 2.0 ± 0.2 s at −100 mV. From Figure 4, it can be taken that the switching of the conductance is reversible; i.e., after switching back to positive voltage, the current rises to its former magnitude.

The addition of PMB to both sides of the membrane abolished the asymmetry of the current–voltage characteristic (Figure 5). Furthermore, the subsequent addition of PMB to the PG side of the membrane resulted in a rapid continuous increase of the membrane current until the membrane finally disrupted (Figure 5). In membrane systems in which the PL side was composed of PC or the PL mixture, the addition of PMB to the PL side had no effect on the bilayer conductance. It is important to note that the asymmetry was not abolished by the addition of PMBN to the PL side (see also Figure 5).

From the traces shown in Figure 3, it might be hypothesized that the observed macroscopic conductance originates from a superposition of a large number of discrete microscopic

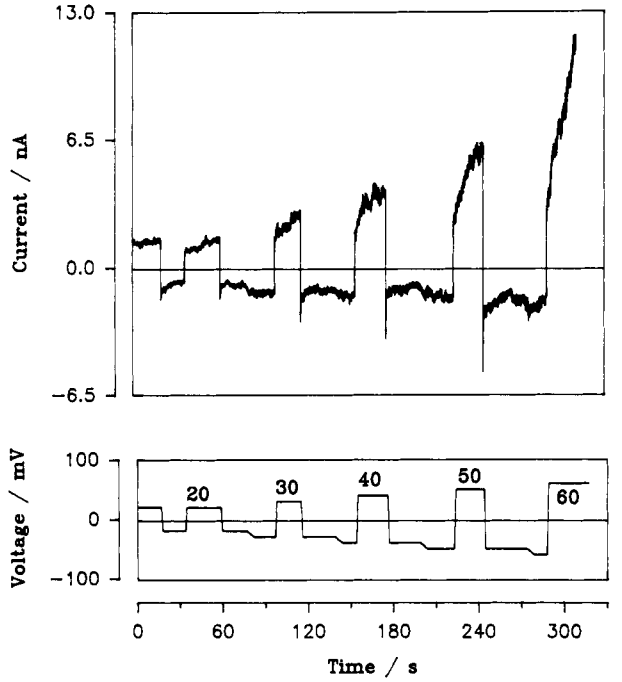

FIGURE 4: Macroscopic current response of PMB-treated bilayers to the applied voltage. Experimental conditions as in Figure 3. Upper trace, membrane current; lower trace, corresponding pulse protocol of the clamp voltage.

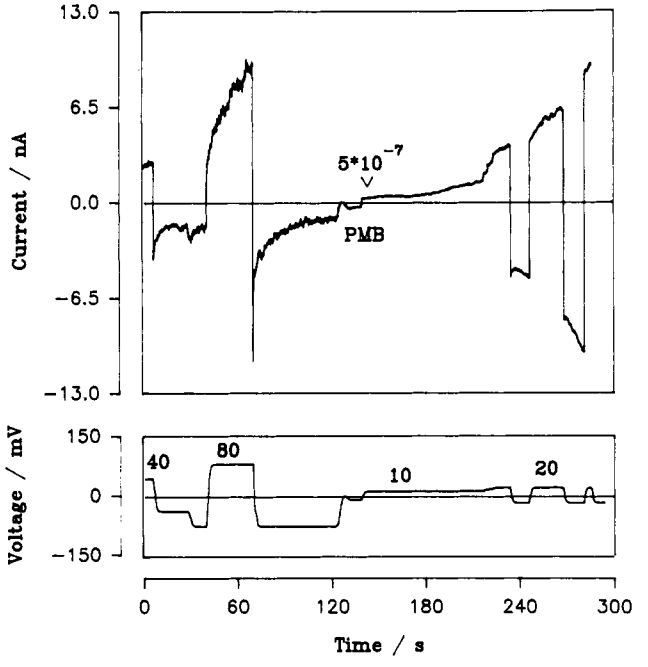

FIGURE 5: Effect of addition of PMB to both compartments on the macroscopic current response as shown in Figure 4. Before the addition of the peptide at the PG side of the membrane, the response on switching of the clamp voltage is as described. In this experiment, at the PL side 5×10^{-7} M PMBN was present in the compartment, which showed no effect on the macroscopic response.

fluctuations similar to those observed in the initial phase following peptide addition. The discrete fluctuations might thus reflect the current through single local perturbations of the normal lipid bilayer structure. The macroscopic current would then be caused by the superposition of currents through a large number of PMB-induced defects in membrane structure. To test this hypothesis, the macroscopic conductance was analyzed with respect to the temporal pattern and to the amplitude of the fluctuations as well as to the mean current. Similar to the experimental conditions in Figure 4, the clamp

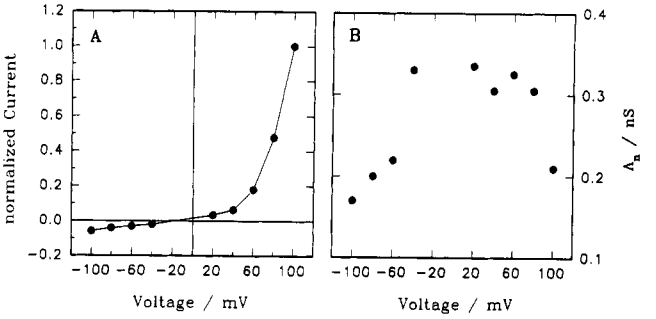

FIGURE 6: (A) Stationary current–voltage characteristic of PMB-treated LPS/PG bilayers. Curves from three independent experiments under identical conditions were normalized to the mean current at +100 mV and averaged. The normalizing factor is 14.5 nS. (B) Conductance variance divided by mean conductance versus clamp voltage.

voltage was switched and kept constant to obtain steady states. Within the steady states, segments of signals with 30-s duration were recorded for various clamp voltages and digitized. From these segments, mean current values, signal variances, and power spectra were calculated.

Figure 6A shows a stationary current–voltage characteristic obtained as an average over three independent experiments with LPS/PG membranes. The amplitudes were normalized to the mean current at +100-mV clamp voltage. At positive voltages, the curve is superlinear but shows a strong rectification at negative voltages. According to basic fluctuation statistics (Neher & Stevens, 1977), the mean conductance, G, of a number of N statistically independent identical lesions with a single conductivity g_0 and an open-state probability p is

$$\bar{G} = g_0 NP \tag{1}$$

and the variance σ_G^2 of the conductance generated by these channels is

$$\sigma_{\bar{G}}^2 = g_0^2 Np(1 - p) \tag{2}$$

Thus, the ratio

$$\Lambda_n = \sigma_{\bar{G}}^2/\bar{G} = g_0(1 - p) \approx g_0 \tag{3}$$

gives (for small open-state probabilities $p \ll 1$) an estimate of the amplitude of the single fluctuations underlying the macroscopic signal. In Figure 6B, Λ_n is plotted versus the clamp voltage. The data were processed from the same recordings which resulted in the macroscopic current–voltage characteristic.

Power spectra under steady-state conditions were estimated by averaging fast Fourier transforms (FFT) from digitized data of recordings. As an example, in Figure 7, a spectrum obtained for a clamp voltage of +80 mV is given. The spectra were of the $1/f^{\alpha}$ type with α being typically 1.5, resulting in a linear slope of the power spectra in a logarithmic plot.

Microscopic Conductance Changes. A sample trace of the recorded discrete fluctuations in the early stage following peptide addition is given in Figure 8A. For a characterization of the fluctuations, their lifetimes, amplitudes, and the dependence of these parameters on the clamp voltage were, as a first approximation, determined by visual inspection and evaluation of the traces (recorded at high time resolution) on a computer screen. Figure 8 shows the results of the analysis for a clamp voltage of +80 mV. The lifetimes of the fluctuations are exponentially distributed as indicated by the linear decline of the lifetime histogram (Figure 8B) in the semilogarithmic plot. From the slope of the regression line, a mean lifetime of 19.9 ms was obtained. Amplitudes (Figure 8C)

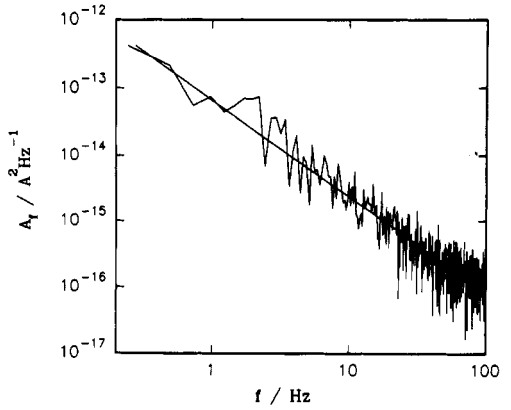

FIGURE 7: Spectral power density versus frequency for a macroscopic membrane current at +80 mV for a PMB-doped LPS/PG bilayer (from signals as in Figure 4). The slope of the spectrum was fitted to $1/f^{\alpha}$ (line), with α being typically 1.5 as determined for various clamp voltages.

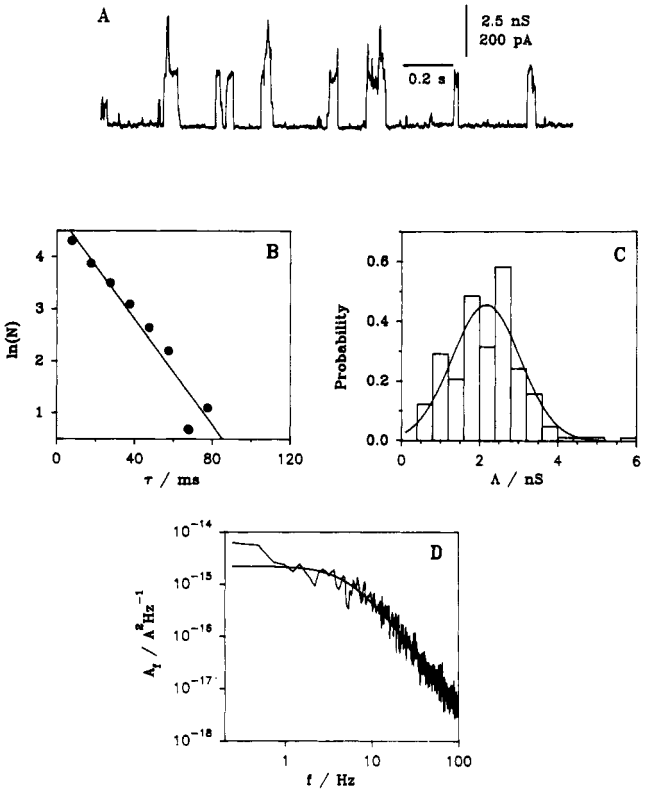

FIGURE 8: Statistical information on the analysis of discrete conductance fluctuations observed immediately after the addition of PMB. Conditions as in Figure 1. (A) Sample trace of single fluctuations recorded at +80-mV clamp voltage. (B) Distribution of fluctuation lifetimes yielding a mean lifetime of 19.9 ms. N is the number of events per 10-ms bin. The total number of events used to construct the histogram was 206. (C) Distribution of fluctuation amplitudes and fit of a Gaussian distribution. The mean conductance is 2.17 nS and the standard deviation 0.87 nS. (D) Power spectrum of the current signal from a PMB-treated membrane at a single fluctuation level. The lower spectral density was fitted to a single Lorentzian according to eq 4 (continuous line).

have a broad distribution with a mean conductivity of 2.2 ± 0.9 nS at +80 mV and the conditions specified in the figure caption.

The above described characterization of traces as in Figure 8A is based on the assumption that the fluctuations can be approximated by rectangular pulses, i.e., that they have flat tops and infinitesimal transition times. Since the observed fluctuations did not show this ideal pattern but were masked in many cases by unspecific erratic fluctuations, this evolution

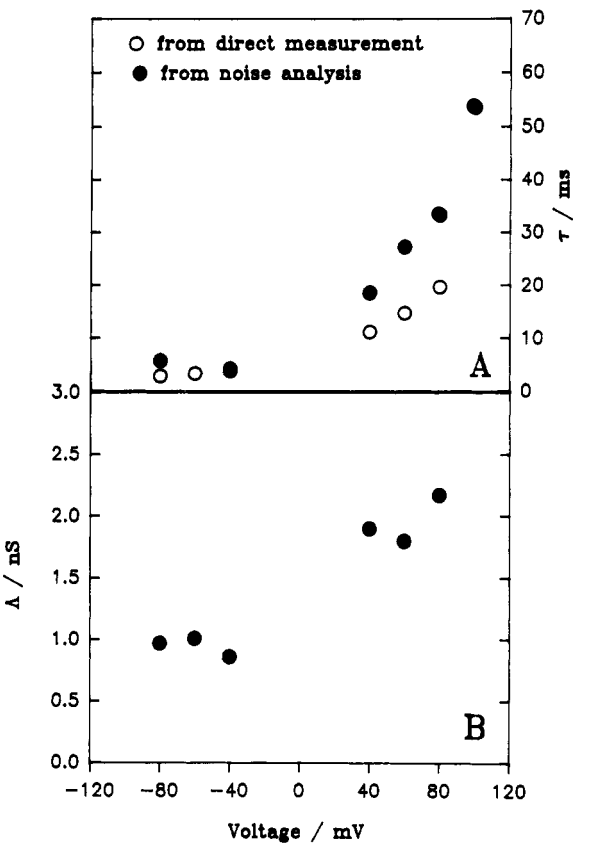

FIGURE 9: Dependence of mean fluctuation lifetimes (A) and mean single fluctuation conductivities (B), respectively, on clamp voltage.

can therefore only be an estimate. Thus, in a second step, an additional check of the lifetimes was provided by analysis of the power spectra of recordings of discrete fluctuations as shown in Figure 8A. As should be expected from the approximated lifetime distribution of the fluctuations, the spectra reasonably fit single Lorentzians; i.e., the amplitude of the power density shows a frequency dependence of the type

$$A(f) = \frac{A_0}{1 + (f/f_c)^2} \text{ with } f_c = \frac{1}{2\pi\tau_m} \qquad (4)$$

where f is the frequency, f_c is the half-power frequency, A_0 is the zero frequency asymptotic value, and τ_m is the mean lifetime of the fluctuations.

Panels A and B of Figure 9 show the dependence of the mean lifetime and of the amplitude of the fluctuations, respectively, on the clamp voltage. The lifetimes decrease drastically from positive to negative voltages. The results obtained from the noise analysis and from the direct measurements are in reasonable agreement, with slightly higher values obtained from the fit of the power spectra.

For the conductance of the fluctuations, typically two values were observed (Figure 9B), approximately 2 nS for positive and around 1 nS for negative voltages, respectively. It is important to note that besides the change in the fluctuation lifetimes, also their frequency of occurrence changed dramatically with clamp voltage. Switching of the clamp voltage between various levels for a membrane with slowly increasing conductance allowed us to obtain a qualitative impression of the dependence of the frequency of the fluctuations on clamp voltage. The traces shown in Figure 10 show that for both polarities the frequency of events is enhanced with increasing clamp voltage.

Film Balance Measurements. Pressure–area isotherms of monolayers prepared from LPS on subphases containing

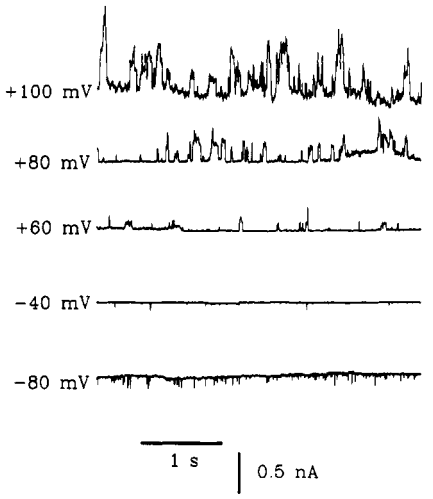

FIGURE 10: Single-fluctuation recordings from one PMB-treated membrane in the initial phase of the conductance increase obtained from switching between the indicated potentials.

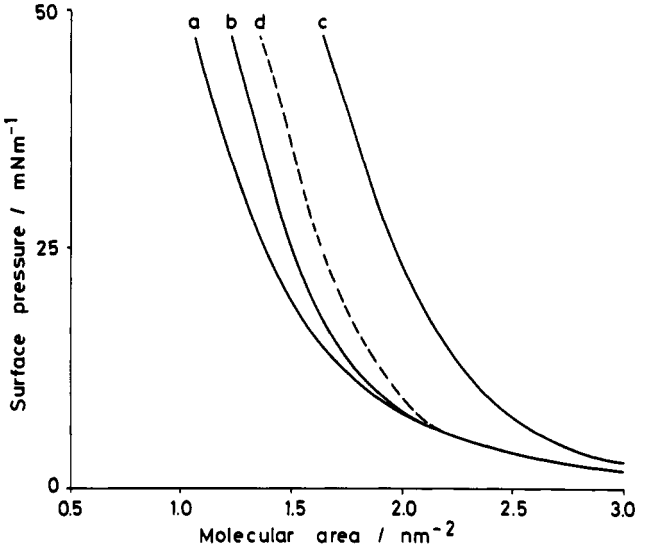

FIGURE 11: Pressure–area curves of LPS monolayers on a 0.1 M NaCl subphase containing various concentrations of PMB or PMBN, respectively: (a) in the absence of antibiotics; (b) 10^{-7} M PMB; (c) 10^{-6} M PMB; (d) 10^{-6} M PMBN.

varying concentrations of PMB and PMBN, respectively, are given in Figure 11. Obviously, at identical concentrations, PMB leads to a larger film expansion than PMBN over the whole pressure range.

DISCUSSION

The activity of PMB on biological membranes has attracted much interest because the peptide is regarded as a small model compound suitable for the study of basic features of lipid/protein interactions. In particular, Gram-negative bacteria are known to be most sensitive to the bactericidal action of PMB, and the lipid matrix, i.e., mainly the outer leaflet of the outer membrane of these organisms, is the primary target of PMB interaction. We have, therefore, reconstituted this particular lipid matrix as an asymmetric LPS/PL bilayer to investigate its interaction with PMB via conductance measurements. The advantage of this experimental approach is the possibility of monitoring functional changes with respect to permeability on a membrane target that mimicks very closely the lipid matrix of the outer membrane of Gram-negative bacteria. Furthermore, it allows us to characterize the size of single lesions induced by membrane-active drugs.

Both the occurrence of discrete conductance fluctuations in the range of nanosiemens (Figures 3, 8, and 10) and the large current noise of the stationary current signal (Figure 3) clearly exclude any carrier mechanism, which has been suggested by Antonov et al. (1976) as an explanation for the enhanced conductivity of painted black lipid membranes, charged by detergents like SDS or Triton, upon interaction with PMB. In contrast to a planar lipid bilayer study by Miller et al. (1978), we were able to detect effects on the bilayer conductivity already upon addition of physiological concentrations of the peptide to one side of the membrane. In contrast to our experimental conditions, Miller et al. and Antonov et al. used exclusively symmetric PL bilayers. The above-mentioned discrepancies may thus result from differences in the lipid compositions of the bilayers employed in the former and our studies, respectively. Of major importance in this context is the surface charge density. The charge density of a condensed R595 LPS monolayer is 4 negative charges/nm^2 whereas that of monolayers from negatively charged phospholipids is approximately half of that value.

Since the amplitudes of the discrete fluctuations (Figure 8) correspond to the transfer of approximately 10^9 ions per second across the bilayer, it should be expected that the conductance results from a local breakdown of the normal lipid bilayer structure, allowing free diffusion of ions. Furthermore, the corresponding structures in the treated membranes must be transient since the discrete conductance fluctuations have only limited lifetimes.

From the conductance of the single fluctuations, the geometrical size of the PMB-induced lesions can be approximated. Assuming that the lesions have a circular geometry filled with an aqueous solution of the same specific conductivity as the external solution (this seems to be reasonable with respect to the magnitude of the conductivity), the radius r of a lesion and its conductivity Λ are related by

$$\Lambda = \pi\sigma r^2/l \qquad (5)$$

where σ is the specific conductivity of the bathing solution and l the membrane thickness. This expression leads to a value of approximately 3 nm for the lesion diameter (l = 5 nm, Λ = 2 nS, and σ = 1400 mS m^{-1}). Both the rapid increase of the ionic conductance after the addition of the drug (Figure 3) and also the approximated size of the PMB-induced lesions account well for the biological activity of PMB. The size of the lesions is sufficiently large to permit also a self-promoted uptake of PMB across the outer membrane (Hancock, 1984).

PMBN is known to lack bactericidal activity (Vaara & Vaara, 1983a) but to sensitize Gram-negative bacteria to various antibiotics by enhancing the uptake of these compounds across the outer membrane (Vaara & Vaara, 1983b), and it was shown to cause also a rapid release of carboxyfluorescein entrapped in PS vesicles (Kubesch et al., 1987). In our experiments, PMBN did not increase bilayer conductance when added alone. It does, however, increase the biological activity of other antibiotics, in particular that of PMB. Perhaps PMBN facilitates the uptake of these compounds via a hydrophobic pathway.

Thus, the experiments with PMBN clearly demonstrate that the presence of the fatty acid and/or the terminal diaminobutyric acid is indispensable for the lethal action of the peptide.

The enhancement of the hydrophobic pathway by PMBN can be explained by its fluidizing effect on lipid bilayer membranes from rough mutant LPS which is comparable to that of PMB [see Kubesch et al. (1987), Beurer et al. (1988), and our own unpublished results from fluorescence polarization measurements]. From this similarity in the fluidizing effect

of PMB and PMBN alone, the differences in their action on the asymmetric planar bilayer system cannot be understood.

However, our film balance measurements with LPS monolayers at the air–water interface clearly revealed that the addition of PMB to the subphase leads to a considerably larger expansion of the monolayer than PMBN at the same concentration (Figure 11). This observation can be explained by the insertion of the fatty acid residue of PMB into the hydrophobic moiety of the LPS monolayer and is in agreement with published monolayer measurements with PL's (Beurer et al., 1988).

A voltage dependence of the conductance induced by polypeptides in planar bilayers is a widely observed phenomenon. Thus, for example, alamethicin (Latorre & Alvarez, 1981), melittin (Kempf et al., 1982), and colicin (Bullock et al., 1990) induce a conductance which increases with increasing field strength across the bilayer, the latter being directed from the peptide-containing toward the peptide-free compartment. This observation has been explained by a field-dependent reorientation of the peptide molecules (Kempf et al., 1982), forcing them into the membrane. The voltage dependence of the PMB-induced conductance, however, shows an opposite dependence on the direction of the electric field and is thus difficult to understand.

That this effect cannot be related to the asymmetry of the planar membrane but rather to the PMB concentration gradient can be determined from Figure 5. It shows that the asymmetry in the membrane current initially observed for a LPS/PG bilayer upon addition of PMB to the LPS side only vanishes upon addition of the same concentration of PMB to the PG side also. In corresponding experiments with asymmetric bilayers made from neutral PL's instead of PG, the subsequent addition of PMB did not provoke vanishing of the current asymmetry, indicating that the electrostatic interaction between PMB and the membrane is a prerequisite for PMB activity.

To further clarify the role of LPS in the interaction of PMB with the bilayer, it should be mentioned that in experiments with symmetric bilayers from neutral phospholipids no conductance changes were induced by PMB. In symmetric PG bilayers, discrete conductance fluctuations of similar amplitude as for the LPS/PL system were observed; however, these effects were much less reproducible, and the characterization was additionally hampered by frequently occurring unspecific membrane breakdown. Similar results were obtained with symmetric LPS membranes. These observations suggest that ion-conducting pathways can be induced by PMB also in symmetric (and asymmetric) membranes from negatively charged phospholipids and this is not an LPS-specific effect.

The high susceptibility of the asymmetric LPS/PL membrane might be explained by the strong tendency of LPS to adopt nonlamellar structures (Seydel & Brandenburg, 1991) and the high surface charge density of R595 LPS monolayers.

The physiological significance of the voltage dependence is not readily understandable, since the cells which are attacked by the peptide are, in general, polarized in a way that the interior is more negative than the outer surface. The electric potential across the outer membrane is assumed to result exclusively from a Donnan equilibrium (Sen et al., 1988). Depending on the composition of the growth medium, negative potentials up to 100 mV on the inner surface of the outer membrane have been determined. However, it has recently been suggested that in the case of mitochondria the potential across the inner membrane might be transduced by capacitive coupling to the outer membrane (Benz et al., 1990). Thus, high positive electrical potentials at the inner side of the outer membrane may exist as contact sites between the inner and outer membrane, and the observed voltage dependence of the activity of PMB may be physiologically meaningful.

A possible explanation for our observations is that PMB molecules, carrying five positive charges, form very stable complexes with more than one LPS molecule each carrying four negative charges. An association or interaction of one membrane-bound PMB molecule with more than one LPS molecule seems to be likely, considering the molecular areas of PMB or LPS, respectively. The cross-sectional area of the peptide ring of PMB was estimated to be approximately 1.23 nm^2 (Theretz et al., 1984), and the molecular area of one LPS R595 molecule is about 1 nm^2 (Brandenburg & Seydel, 1984). These complexes would have a net negative charge and would thus react in the expected way to the electric field across the membrane and could thus give rise to the observed voltage dependence. This explanation is furthermore confirmed by the observation that the peptide shows a normal orientational behavior (in response to an electric field across the membrane) for membranes composed with a less negative charge density as shown by Miller et al. (1978). These authors demonstrated with polarographic measurements on monolayers from bacterial total lipid extract (charge density approximately 0.5/nm^2) an enhancement of the destabilizing effect of PMB for an electric field across the membranes, positive in direction of the adsorption side.

Our data are basically in accordance with the assumption that the macroscopic conductance results from the superposition of a large number of single fluctuations as observed directly following peptide addition. According to eq 1, the mean conductance depends on the conductance of the individual lesions and on their number. Thus, the observed voltage dependence might be caused by a voltage dependence of either one of these two parameters. From the macroscopic measurements, it seems likely that the enhanced conductivity for large positive clamp voltages results from an increasing number of lesions in the membrane since the ratio of the noise variance to the mean current shows only small changes upon variation of the voltage (Figure 6B). In agreement with this, we found that the amplitudes of the discrete single fluctuations vary only slightly with the clamp voltage (Figure 9B) but that the frequency of occurrence of the fluctuations is enhanced with increasing electric field strength (Figure 10). However, the amplitudes of the single fluctuations as estimated from the macroscopic conductance measurements (Figure 6B) as well as the power spectra of signals computed from macroscopic currents (Figure 7) show a considerable mismatch with the corresponding features of the single fluctuations (Figure 8). A possible explanation for this mismatch is that the precondition for the analysis of the macroscopic current noise, i.e., the individual lesions have to be statistically independent, is not fulfilled. A similar discrepancy between single-channel and macroscopic conductance measurements has also been observed for membranes doped with gramicidin (Kolb & Bamberg, 1977).

The following considerations suggest that the discrete conductance fluctuations upon addition of PMB measured under voltage-clamp conditions result rather from a derangement of membrane lipids than from the formation of structural channels in the sense of a protein-lined pore. (i) The molecular geometry of PMB: Molecular models (Hartmann et al., 1977) show that the peptide is too small to span a whole bilayer. (ii) The critical concentration dependence for the induction of the conductance changes: Pore-

forming peptides like alamethicin show an overlinear dependence of the conductivity on peptide concentration with a high power dependence (exponents >6) (Latorre & Alvarez, 1981). These results are interpreted as the formation of multimeric pores by aggregation of large numbers of monomers. However, even very low antibiotic concentrations are still able to induce single-channel activities in planar bilayers. Our finding of a threshold concentration below which no activity at all is found is not compatible with the idea of multimeric pores.

Hartmann et al. (1977) have proposed a model for the mechanism of action of PMB which, in brief, involves the following steps:

PMB binds to negatively charged lipids and causes phase separation between free lipid and PMB-bound lipid. This arrangement should finally result in a local curvature of the lipid bilayer and the formation of a pore in the center of polymyxin/lipid domains. With our experimental approach we could, for the first time, demonstrate the induction of porelike lesions by PMB in a lipid bilayer. From the critical concentration dependence, it seems to be attractive to postulate that the action of PMB is related to that of detergents (Helenius & Simons, 1975; Schlieper & de Robertis, 1977; Glaser et al., 1988).

At a critical PMB concentration at the bilayer surface, a local structural transition spontaneously takes place in the way that micelles—most likely mixed micelles from PMB and LPS (or other negatively charged lipids) due to the tight electrostatic interaction—are formed. The formation of the micelles is accompanied by local perturbations of the normal lipid bilayer structure leading to the occurrence of transmembrane lesions which permit the observed free diffusion of ions. Furthermore, it is likely that the size distribution of the micelles is rather narrow and, therefore, explains the relatively high reproducibility of the amplitude of the discrete conductivity fluctuations.

The transient character of the lesions may be understood in terms of a critical equilibrium between the bilayer and those structures through which the ionic permeability occurs.

ACKNOWLEDGMENTS

We gratefully acknowledge many fruitful discussions with Dr. E. Th. Rietschel. We are also indebted to Chr. Hamann, G. von Busse, and D. Koch for their technical assistance and to M. Lohs and B. Köhler for the preparation of the drawings and photographs, respectively.

Registry No. Polymyxin, 1404-26-8.

REFERENCES

Antonov, V. F., Korepanova, E. A., & Vladimirov, Y. A. (1976) *Stud. Biophys. 58*, 87.

Benz, R., Kottke, M., & Brdiczka, D. (1990) *Biochim. Biophys. Acta 1022*, 311.

Beurer, G., Warncke, F., & Galla, H.-J. (1988) *Chem. Phys. Lipids 47*, 155.

Bezanilla, F. (1985) *Biophys. J. 47*, 437.

Boggs, J. M., & Rangaraj, G. (1985) *Biochim. Biophys. Acta 816*, 221.

Brandenburg, K., & Seydel, U. (1984) *Biochim. Biophys. Acta 775*, 225.

Bullock, J. O., Armstrong, S. K., Shear, J. L., Lies, D. P., & McIntosh, M. A. (1990) *J. Membr. Biol. 114*, 79.

Galanos, C., Lüderitz, O., & Westphal, O. (1969) *Eur. J. Biochem. 9*, 245.

Glaser, R. W., Leikin, S. L., Chernomordik, L. V., Pastushenko, V. F., & Sokirko, A. I. (1988) *Biochim. Biophys. Acta 940*, 275.

Hancock, R. E. W. (1984) *Annu. Rev. Microbiol. 38*, 237.

Hartmann, W., Galla, H. J., & Sackmann, E. (1977) *Biochim. Biophys. Acta 510*, 124.

Helenius, A., & Simons, K. (1975) *Biochim. Biophys. Acta 415*, 29.

HsuChen, C. C., & Feingold, D. S. (1973) *Biochemistry 12*, 2105.

Imai, M., Inoue, K., & Nojima, S. (1975) *Biochim. Biophys. Acta 375*, 130.

Kempf, C., Klausner, R. D., Weinstein, J. N., Van Renswoude, J., Pincus, M., & Blumenthal, R. (1982) *J. Biol. Chem. 257*, 2469.

Kolb, H.-A., & Bamberg, E. (1977) *Biochim. Biophys. Acta 464*, 127.

Kubesch, P., Boggs, J., Luciano, L., Maass, G., & Tümmler, B. (1987) *Biochemistry 26*, 2139.

Latorre, R., & Alvarez, O. (1981) *Physiol. Rev. 61*, 77.

Miller, I. R., Bach, D., & Teuber, M. (1978) *J. Membr. Biol. 39*, 49.

Mushayakarara, E., & Levin, I. W. (1984) *Biochim. Biophys. Acta 769*, 585.

Neher, E., & Stevens, C. F. (1977) *Annu. Rev. Biophys. Bioeng. 6*, 345.

Osborn, M. J., Gander, J. E., Parisi, E., & Carson, J. (1972) *J. Biol. Chem. 247*, 3962.

Peterson, A., Hancock, R. E. W., & McGroarty, E. J. (1985) *J. Bacteriol. 164*, 1256.

Ranck, J. L., & Tocanne, J. F. (1982) *FEBS Lett. 143*, 175.

Schindler, M., & Osborn, M. J. (1979) *Biochemistry 18*, 4425.

Schindler, P. R. G., & Teuber, M. (1975) *Antimicrob. Agents Chemother. 8*, 95.

Schlieper, P., & de Robertis, E. (1977) *Arch. Biochem. Biophys. 184*, 204.

Sen, K., Hellman, J., & Nikaido, H. (1988) *J. Biol. Chem. 263*, 1182.

Seydel, U., & Brandenburg, K. (1991) in *Bacterial Endotoxic Lipopolysaccharides* (Morrison, D. C., & Ryan, J. L., Eds.) Vol 1 (in press).

Seydel, U., Schröder, G., & Brandenburg, K. (1989) *J. Membr. Biol. 109*, 95.

Sixl, F., & Watts, A. (1985) *Biochemistry 24*, 7906.

Storm, D. R., & Rosenthal, K. (1977) *Annu. Rev. Biochem. 46*, 723.

Teuber, M. (1974) *Arch. Microbiol. 100*, 131.

Theretz, A., Theissie, J., & Tocanne, J. F. (1984) *Eur. J. Biochem. 142*, 113.

Vaara, M., & Vaara, T. (1983a) *Antimicrob. Agents Chemother. 24*, 114.

Vaara, M., & Vaara, T. (1983b) *Nature 303*, 526.